BILINGUAL PUBLISHING GROUP

Organic Polymer Material Research

https://journals.bilpubgroup.com/index.php/opmr

ARTICLE

Synthesis and Characterization of Benzobisoxazole-based Conjugated Polymers for Organic Photodetectors

Myeong In Kim, WonJo Jeong*

Department of Organic and Nano Engineering, and Human-Tech Convergence Program, Hanyang University, 222 Wangsimni-ro, Seongdong-gu, Seoul, 04763, Republic of Korea

ABSTRACT

Benzo[1,2-d:4,5-d']bis(oxazole) (BBO) is a conjugated building block that can be easily synthesized for the development of organic optoelectronic polymers. Here, the authors synthesized BBO-based polymers, P1 and P2, by coupling BBO with thiophenes for use in organic photodetectors (OPDs). The optical characteristics of P1 and P2 make them suitable for OPDs, as they selectively absorb the green light with a narrow bandwidth in the range of 500–600 nm. The OPD devices were fabricated by making a bulk heterojunction active layer between the synthesized polymers and a nonfullerene acceptor, IDIC. P1-based devices showed slightly higher responsivity (R) of 0.169 A/W than 0.112 A/W of P2-based devices. However, the P2-based device was higher than D^* value of the P1-based under 100 μW/cm^2, which was due to the influence of excessive thiophene units that had low dark current density.

Keywords: Organic photodetector; p-type polymer; Conjugated polymer; Alkylthiophene π-spacer; Benzobisoxazole

1. Introduction

Organic photodetectors (OPDs) have been given attention due to their unique characteristics such as high absorption coefficient, tunable absorption region and broadness, light weight, and solution-processibility. Thus, OPDs are considered to be one of the promising options for optical sensors and communications in wearable, portable, and light-weight electronic devices [1–6]. In the OPD devices, the photoconductive layer has the greatest influence on the bandwidth, photocurrent density (J_{ph}), dark current density (J_d), responsivity (R) and specific detectivity

*CORRESPONDING AUTHOR:
WonJo Jeong, Department of Organic and Nano Engineering, and Human-Tech Convergence Program, Hanyang University, 222 Wangsimni-ro, Seongdong-gu, Seoul, 04763, Republic of Korea; Email: zozosy@hanyang.ac.kr

ARTICLE INFO
Received: 31 December 2023 | Revised: 24 January 2024 | Accepted: 20 February 2024 | Published Online: 27 February 2024
DOI: https://doi.org/10.30564/opmr.v5i2.6192

CITATION
Kim, M.I., Jeong, W., 2024. Synthesis and Characterization of Benzobisoxazole-based Conjugated Polymers for Organic Photodetectors. Organic Polymer Material Research. 5(2): 11–25. DOI: https://doi.org/10.30564/opmr.v5i2.6192

(D^*), and thus the development of photoconductive polymer is highly important for OPDs [7]. Previous research has studied increasing both the R and D^* values and decreasing J_d values.

Xai et al. fabricated p-n bulk heterojunction organic photodiodes (OPDs) using a small-molecule donor based on squaraine and a non-fullerene acceptor (NFA) composed of polycyclic aromatic rings. They successfully achieved red-selective OPDs with a D^* value of 4.70×10^{11} Jones, unbiased, and a full width at half maximum (FWHM) of 186 nm [3]. Kim et al. synthesized phthalocyanine-based conjugated small molecules. They exhibited a D^* value of 1.0×10^{12} Jones under 530 nm light-emitting diode light of 0.1 mW/cm^2 at –2 V bias. In addition, in the dynamic characteristics of the OPD, they were investigated that the –3 dB cut-off frequency of CuPc-HT:$PC_{71}BM$ devices was extremely high at 0.1 MHz, and the signal response time was ultrafast at 9 μs [8]. Kang et al. synthesized p-type donor PSBOTz and n-type nonfullerene acceptor (NFA) T2-OEHRH. OPDs fabricated of PSBOTz and T2-OEHRH exhibited a great R value of 0.31 A/W and D^* value of 2.04×10^{13} Jones –2 V bias [9]. In addition, it showed green selective OPD in the full width at a half-maximum (FWHM) region of 230 nm. Jeong et al. synthesized a BBO-based conjugated polymer donor which was named as PBB. The halogen-free solvent processed OPDs were developed with outstanding R value of 0.385 A/W and D^* value of 1.33×10^{13} Jones, respectively, at –1 V bias under 532 nm light illumination [10]. After that, they incorporated thiophene π-spacer in a conjugated polymer donor, and found the correlation between J_d and hole charge-transfer (CT) state, which was informative to understand and reduce J_d in the OPDs [11]. Jeong et al. synthesized cyclopentadithiophene (CPDT)-based red and near-infrared conjugated polymer donor. By including a thienothiophene (TT) ring into the polymers, a stable quinoid structure was maintained, showing wavelength absorption at 700–900 nm [12]. They showed high performance with D^* value of 1.14×10^{12} Jones at –1 V bias. Kim et al. developed NDI-based and PDI-based n-type polymers with nonconjugated spacer. To decrease J_d, nonconjugated spacers with various chain lengths, ether and thioether-mediated nonconjugated spacers were synthesized. They exhibited highly low J_d value of 5.1×10^{-9} A/cm^2 and D^* value of 1.0×10^{12} Jones at –1 V bias [13]. Kim et al. synthesized a PDI-based small molecule acceptor. Among three small molecules, I-NPDI, including indacenodithiophene (IDT), showed better charge transport and suppressed J_d characteristics. They exhibited R value of 0.231 A/W, low J_d value of 5.92×10^{-10} A/cm^2 and D^* value of 8.09×10^{12} Jones at –2 V bias [14].

Benzo[1,2-d:4,5-d'] bis(oxazole) (BBO) moiety, which has a linear alkyl chain, has many advantages for building a conjugated polymer donor. Firstly, it is a polynuclear heterocyclic aromatic ring, and thus it has a planar structure and is advantageous for π-π stacking, facilitating efficient charge transport of the polymers. Secondly, this aromatic ring itself contains alkyl side chains, which increase the solubility of the polymer [10,11]. We expected great performance, which was expanded π-specer, by a BBO moiety.

In this study, we synthesized two green-light absorption conjugated polymer donor, poly[2,6-dioctyl-4,8-bis(4-octylthiophen-2-yl)benzo[1,2-d:4,5-d'] bis(oxazole)-alt-2,5-thiophene] (P1) and poly[2,6-dioctyl-4,8-bis(4-octylthiophen-2-yl)benzo[1,2-d:4,5-d']bis(oxazole)-alt-2,2'-bithiophene] (P2), by Stille coupling reaction between the brominated BBO-based monomer (compound 7) and the stannylated thiophene-based monomers (compound 5 and 8) as shown in **Scheme 1**. The polythiophenes are the most well-known conjugated donors. It shows promising charge transporting properties in the film states [15,16]. In addition, alkylated thiophene can lower dark current density [11]. Thus, the combination between thiophenes and BBO can give a possibility to build conjugated polymer donor for OPDs, and the number of thiophene rings was adjusted in the synthesized two polymers (P1 and P2).

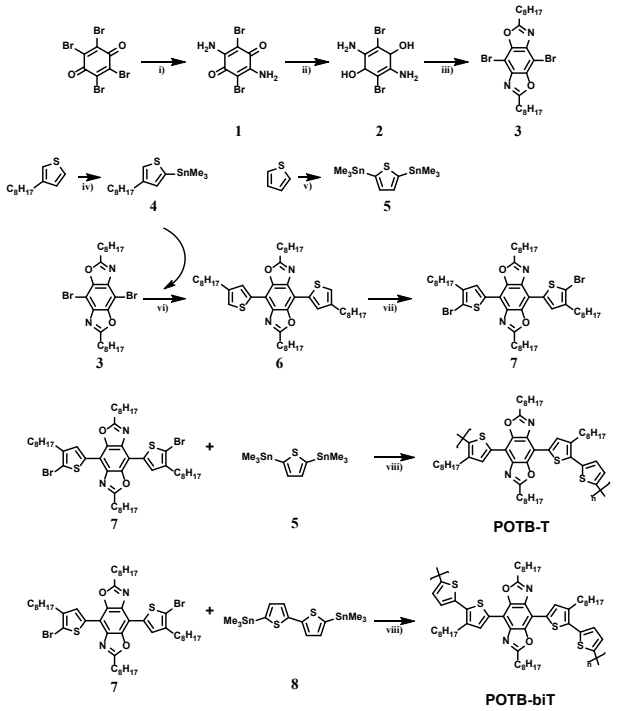

Scheme 1. Synthesis of P1 and P2 polymers. i) 27% NH_4OH solution, 2-methoxyethyl acetate, 100 °C 3.0 hours reaction. ii) $Na_2S_2O_4$ (2.0 M in water) , Ethanol, 55 °C 2.0 hours reaction. iii) Poly(trimethylsilyl phosphate), nonanoyl chloride, *o*-DCB, 90 °C, 3 day reaction. iv–v) n-BuLi (2.5 M in hexane), trimethyltin chloride (1.0 M in THF), –78 °C iv), 40 °C v), overnight reaction. vi) 5-Trimethylstannyl-3-octylthiophene, tris(dibenzylideneacetone)dipalladium ($Pd_2(dba)_3$), Tri(o-tolyl) phosphine (p-(o-tolyl)$_3$), toluene, 116 °C, overnight reaction. vii) N-bromosuccinimide (NBS), DMF, R.T., overnight reaction. viii) Compound 5, 7, 8, tetrakis(triphenylphosphine)palladium(0), toluene, 116 °C, 3.0 hours reaction.

The OPD devices were fabricated by blending a conjugated polymer donor (P1 or P2) and a nonfullerene acceptor (IDIC). P1-based devices showed the best OPD performance with a R of 0.17 A/W, J_d of 1.47×10^{-7} A/cm^2 and D^* of 7.78×10^{11} Jones at –1 V bias, whereas P2-based devices showed a R of 0.11 A/W and J_d of 7.41×10^{-8} A/cm^2 and D^* of 7.28×10^{11} Jones. However, when the P2-based devices showed under 100 μW/cm^2 light intensity, D^* was measured to be higher than P1-based devices. Additionally, we analyzed the P1 and P2 through external quantum efficiency (EQE) and space charge limited current (SCLC).

2. Experimental section

2.1 Materials synthesis

Synthesis of 2,5-diamino-3,6-dibromocyclohexa-2,5-diene-1,4-dione

Bromanail (10.0 g, 23.6 mmol) was dissolved in 2-methoxyethyl acetate (50.0 mL) at 100 °C and stirred fro 1 hour. The solution was cooled to room temperature, and 27% NH_4OH (4.8 mL) was added dropwise. The resulting mixture was stirred at 100 °C for 3 hours. Afterward, the mixture was washed with water and acetone, followed by filtration. The obtained filtrate was dried under vacuum. Resulting in a yield of (5.54 g, 79.14%). Due to the compound limited solubility, it was used without further purification or analysis.

Synthesis of 2,5-diamino-3,6-dibromobenzene-1,4-diol

2,5-diamino-3,6-dibromocyclohexa-2,5-diene-1,4-dione (18.6 mmol, 5.54 g) was stirred in 60 mL of ethanol and 15 mL of distilled water under nitrogen at 55 °C. $Na_2S_2O_4$(46.5 mmol, 8.0 g) dissolved in 80 mL of distilled water was added dropwise and the mixture stirred for 1 hour. The reaction mixture was allowed to cool to room temperature the precipitate was filtered and washed with distilled water and cold ethanol. The solid was dried under vacuum to give the product (5.54 g, 99%). Because of the insolubility and air sensitivity of synthesis of 2,5-diamino-3,6-dibromobenzene-1,4-diol. It was used immediately without further purification or analysis.

Synthesis of 4,8-dibromo-2,6-dioctylbenzo[1,2-d:4,5-d']bis(oxazole)

Poly(trimethylsilyl phosphate) (13.0 g) and nonanoyl chloride (10.0 g, 44.64 mmol) were dissolved in *o*-DCB (50 mL). The solution was degassed by bubbling argon through it for 30 minutes and added the solution in a N_2 atmosphere flask containing 2,5-diamino-3,6-dibromobenzene-1,4-diol (5.54 g, 18.6 mmol). The mixture was heated to 90 °C for 72 hours. The solution is concentrated by vacuum dis-

tillation of the *o*-DCB. The resulting crude product was purified by column chromatography. The resulting white solid was recrystallized using DCM/methanol to given compound 3 (6.37 g, 63.1%). ^{1}H-NMR (600 MHz, $CDCl_3$) δ: 3.010 (m, 4H), 1.924 (dt, 4H), 1.444–1.276 (m, 20H), 0.879 (m, 6H).

Synthesis of 5-Trimethylstannyl-3-octylthiophene

3-octylthiophene (2.0 g, 10.2 mmol) was dissolved in anhydrous THF (20 mL). Dropwise n-Butyllithium (2.5 M in hexane) (6.2 mL, 15.3 mmol) at –78 °C and stirring for 2 hours. After the solution was stirred for 1 hour at room temperature. The solution was cooled down to –78 °C, and trimethyltin chloride (1.0 M in THF) (30 mL, 30.6 mmol) was added one shot injection and stirred overnight under N_2 atmosphere. The reaction mixture was extracted with diethyl eher, washed water, and dried over $MgSO_4$. After removing the solvent to afford product pale liquid (3.66 g, 100%) NMR (600 MHz, $CDCl_3$) δ: 7.201 (s, 1H), 7.013 (s, 1H), 2.646 (t, 2H), 1.631 (q, 2H), 1.349–1.250 (m, 10H), 0.885 (t, 3H), 0.354 (m, 9H).

Synthesis of 2,5-bis(trimethylstannyl)thiophene

Thiophene (1.0 g, 11.88 mmol) and TMEDA (3.04 g, 26.14 mmol) were dissolved in anhydrous hexane (45.0 mL) under N_2 atmosphere. Dropwise n-Butyllithium (2.5 M in hexane) (10.5 mL, 26.14 mmol) at room temperature and stirring for 1.0 hour. After the solution was stirred for 1 hour at 60 °C. The solution was cooled down to 0 °C, and trimethyltin chloride (1.0 M in THF) (30 mL, 29.7 mmol) was added one shot injection and stirred overnight. The reaction mixture was extracted with diethyl eher, washed water, and dried over $MgSO_4$. After removing the solvent to afford product white solid (2.75 g, 56.5%) ^{1}H NMR (600 MHz, $CDCl_3$) δ: 7.317 (d, 2H), 0.366 (s, 18H).

Synthesis of 2,6-dioctyl-4,8-bis(4-octylthiophen-2-yl) benzo[1,2-d:4,5-d']bis(oxazole)

4,8-dibromo-2,6-dioctylbenzo[1,2-d:4,5-d'] bis(oxazole) (2.0 g, 3.69 mmol), tris(dibenzylideneacetone)dipalladium(0) (102.0 mg, 0.11 mmol), tri(o-tolyl)phosphine (p-(o-tolyl)$_3$) (112.0 mg, 0.37 mmol) were dissolved in toluene (40.0 mL). The mixture was added 5-Trimethylstannyl-3-octylthiophene (4.0, 11.06 mmol) in a N_2 atmosphere flask. The mixture was heated to 110 °C for an overnight reaction. The reaction mixture was extracted with methylene chloride (M.C.), washed water, and dried over $MgSO_4$ after removing the solvent. The resulting crude product was purified by column chromatography (eluent is M.C.: Hex = 1:3) and recrystallized to afford product as a yellow solid (1.91 g, 66.8%). ^{1}H-NMR (600 MHz, $CDCl_3$) δ: 8.146 (s, 2H), 7.099 (s, 2H) 3.089 (t, 4H), 2.729 (t, 4H), 2.000 (q, 4H), 1.719 (q, 4H), 1.531–1.297 (m, 40H), 0.883 (m, 12H).

Synthesis of 2,6-dioctyl-4,8-bis(5-bromo-4-octylthiophen-2-yl) benzo[1,2-d:4,5-d']bis(oxazole)

2,6-dioctyl-4,8-bis(4-octylthiophen-2-yl) benzo[1,2-d:4,5-d'] bis(oxazole) (1.8 g, 2.33 mmol) was dissolved in DMF (50.0 mL). The mixture added the N-bromosuccinimide(NBS) (0.91 g, 5.12 mmol) at an overnight reaction and room temperature. The reaction mixture was extracted with M.C., washed water, and dried over $MgSO_4$. After removing the solvent and purified by purified by column chromatography (eluent is M.C.: Hex = 1:3). Recrystalized to afford product as a yellow solid. (2.04 g, 94.2%) ^{1}H-NMR (600 MHz, $CDCl_3$) δ: 7.965 (s, 2H), 3.075 (t, 4H), 2.672 (t, 4H), 1.988 (q, 4H), 1.688 (q, 4H), 1.527-1.297 (40H), 0.885 (m, 12H).

Polymerization of P1(POTB-T)

2,6-dioctyl-4,8-bis(5-bromo-4-octylthiophen-2-yl) benzo[1,2-d:4,5-d']bis(oxazole) (0.204 g, 0.219 mmol), 2,5-bis(trimethylstannyl)thiophene (0.090 g, 0.219 mmol) and tetrakis(triphenylphosphine)palladium(0) (12.4 mg, 0.011 mmol) were dissolved in toluene (4.5 mL). The mixture was heated at 120 °C and 2.0 hours reaction. After polymerization, the polymer was washed by soxhlet extraction with methanol, acetone, and chloroform. The polymer solution in chloroform was filtered through a Celite filter. P1 was obtained by reprecipitation from methanol (100.0 mg, 53.4%). Elemental Anal. Calcd $C_{52}H_{74}N_2O_2S_3$: C:73.02; H:8.72; N: 3.28; O:3.74;

S:11.24. Found: C, 72.6; H, 8.49; N, 3.17; S, 11.4.

Polymerization of P2(POTB-biT)

P2 was polymerized using the same P1 polymer. The polymerization involved 2,6-dioctyl-4,8-bis(5-bromo-4-octylthiophen-2-yl) benzo[1,2-d:4,5-d']bis(oxazole) (200.0 mg, 0.215 mmol), 5,5'-bis(trimethylstannyl)-2,2'-bithiophene (105.6 mg, 0.215 mmol), tetrakis(triphenylphosphine)palladium(0) (12.4 mg, 0.011 mmol), and toluene (4.2 mL). The mixture was then refluxed at 120 °C for 16.0 hours. P2 was obtained by recrystallization from methanol (123.1 mg, 61.1%). Elemental Anal. Calcd $C_{56}H_{76}N_2O_2S_4$: C:71.75; H:8.17; N: 2.99; O:3.41; S:13.68. Found: C, 71.6; H, 8.10; N, 2.95; S, 13.5.

2.2 Device fabrication and characterization

Patterned indium-doped tin oxide (ITO)-coated glass substrates were used as the bottom transparent electrode. ITO substrates were cleaned through sonication with acetone, distilled water, and ethanol sequentially, each for 20 minutes. The remaining solution was then removed using N_2 blowing. The ZnO precursor solution was prepared by dissolving 0.45 M of zinc acetate dehydrate and 0.45 M of monoethanolamine in 2-methoxyethanol at 60 °C for 3 hours. After cooling, the precursor solution was aged overnight. Before the coating process, ITO substrates were subjected to UV-O_3 treatment for 20 minutes. The prepared ZnO precursor solution was spin-coated onto the ITO at 3000 rpm for 30 seconds. The ZnO-precursor-coated ITO substrates were thermally annealed at 220 °C for 10 minutes. The BHJ photoconductive layer consisted of donor polymers (P1 and P2) and acceptor (IDIC) with a ratio of 1:1.5. The concentration of the blended solution in chloroform was 25 mg/mL. After stirring for 3 hours, the blended solution was spin-coated onto the ZnO-coated ITO at 1000 rpm for 40 seconds. The fabrication of the BHJ conductive layer was carried out in an Ar-filled glovebox. MoOx and Ag were thermally deposited under high vacuum conditions, with thicknesses of 8 nm and 100 nm, respectively. MoO_x served as the hole-transporting layer (HTL), while Ag was used as the top electrode.

3. Results and discussion

3.1 Synthesis and characterization of the polymers

The synthetic routes for the P1 and P2 are shown in **Scheme 1**. Compounds 1–3 were synthesized according to the previous literature [10,11,17]. 5-Trimethylstannyl-3-octylthiophene (compound 4) and 2,5-bis(trimethylstannyl)thiophene (compound 5) were synthesized from thiophene and 3-octylthiophene, respectively, by the continuous process of lithiation using BuLi and distannylation using trimethyltin chloride. Compound 6 was obtained via the Stille cross-coupling reaction between compound 3 and 2-trimethylstannyl thiophene in the presence of a palladium catalyst. Subsequently, the bromination of compound 7 using NBS resulted in the final monomer 7. 5,5'-Bis(trimethylstannyl)-2,2'-bithiophene (compound 8) was purchased from Sigma-aldrich Inc. P1 and P2 were synthesized by Stille cross-coupling reaction of monomer 7 with co-monomer 5 and 8, respectively, in the presence of a palladium catalyst.

The molecular weights of the synthesized polymers were analyzed by gel permeation chromatography (GPC). The number average molecular weights of P1 and P2 were 5,600 and 4,800 Da, respectively, and the corresponding weight average molecular weights were 7,200 and 9,600 Da, respectively (**Figures S5 and S6**). Both polymers showed good solubility in common organic solvents such as chloroform, toluene and tetrahydrofuran (THF).

The ultraviolet-visible spectra of P1 and P2 were analyzed in both solution and film states. As shown in **Figure 1a**, the maximum absorption wavelengths (λ_{max}) of P1 and P2 were 477 and 476 nm, respectively, in the diluted solution. Regardless of the number of thiophene rings, two polymers showed similar absorption behaviors in the solution. In the film state, as shown in **Figure 1b**, λ_{max} was 555 and 602 nm for P1, and 553 and 596 nm for P2. The optical properties are shown in **Table 1**. The absorption bandwidth

of P1 and P2 was increased when changing from solution to film. This indicates that the intermolecular ordering of P1 and P2 was enhanced in the film state. The two polymers also exhibited quite similar absorption behaviors in the film states with a strong green light absorbance. P1 polymer shows a stronger shoulder peak. Because the length of the polymer unit is short, which strengthens the **π-π** stacking between polymers. But This indicates that the effective π-conjugation was already saturated at P1, and the additional thiophene ring in P2 had a negligible effect on absorbance. The optical bandgaps (E_g) of P1 and P2 were calculated from the absorption onset wavelength of the polymer film, and all the polymers had similar values of ~ 2.0 eV.

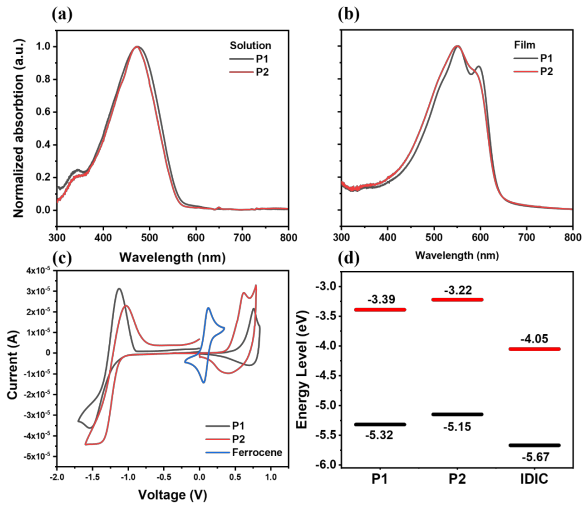

Figure 1. Characterization of the POTB-T, POTB-TT polymers: a, b) absorption spectra of the PBBOCPDT, POTBCPDT polymers in solution and film states and c) cyclic voltammograms of POTB-T, POTB-TT. d) Energy level diagram of used materials.

The energy levels of the synthesized polymers were analyzed by cyclic voltammetry (CV) (**Figure 1c**). The highest occupied molecular orbital (HOMO) and lowest unoccupied molecular orbital (LUMO) energy levels were extracted from the oxidation onset potential (E_{ox}) and the reduction onset potential (E_{red}), respectively, based on the ferrocene reference electrode. The E_{ox} of P1 and P2 were 0.60 and 0.43 V from the equation: E_{HOMO} = [4.8 + (E_{ox} – $E_{1/2(ferrocene)}$)] eV, respectively [18]. The corresponding HOMO energy level (E_{HOMO}) was –5.32 and –5.15 eV, respectively. The LUMO energy level (E_{LUMO}) of P1 and P2 were –3.39 and –3.22 eV, respectively, which was calculated from the equation [E_{LUMO} = (E_{HOMO} – E_g^{opt})]. The HOMO energy level of P1 was lower than that of P2 because P1 has a lower content of electron donating thiophene than P2 [19,20]. The electrochemical properties are shown in **Table 1**.

3.2 OPD properties

The BHJ OPDs were fabricated with a structure of ITO/ZnO/photoconductive layer/MoOx/Ag. The *p-n* photoconductive layer is composed of P1:IDIC or P2:IDIC (1:1.5 w/w%). Under the collimated 532 nm LED illumination, current density-voltage (*J-V*) curves are measured by varying incident power intensities (**Figure 2**). Both devices show typical *p-n* junction photodiode characteristics by forming a reverse-saturation current density in the third quadrant of the *J-V* curves. The *R* values of devices were calculated from the *J-V* curve in the third quadrant, which indicates the ratio of J_{ph} to the power of incident light (P_{in}) as shown in Equation (1) [21,22].

Table 1. Optical and electrochemical properties of P1 and P2.

Polymer	Λmax (nm)		OnsetUV	Optical band gap (eV)	EHOMOCV (eV)	ELUMO (eV)
	Solution	Film				
P1	477	555,602	643	1.93	–5.32	–3.39
P2	476	553,596	638	1.93	–5.15	–3.22

$$R\ (\mathrm{A/W}) = \frac{J_{ph}}{P_{in}} \quad (1)$$

The specific detectivity (D^*) values were calculated from the measured R values and the J_d values from the J-V curves by following Equation (2), where q is the elementary charge.

$$D^*\left(\mathrm{cm} \cdot Hz^{-0.5}W^{-1}, \mathrm{Jones}\right) = \frac{R}{\sqrt{2qJ_d}} \quad (2)$$

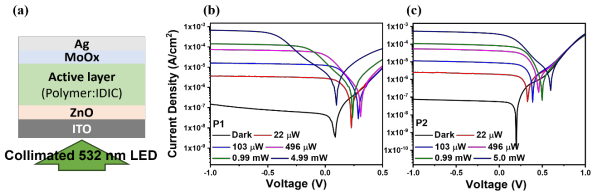

Figure 2. (a) Schematic illustration of fabricated OPD. J-V curves under 532 nm LED illumination of (b) P1:IDIC and (c) P2:IDIC.

P1-based devices showed higher J_{ph} and R values than those of P2-based devices. Because D^* reflects both R and J_d characteristics, it is important to assess the performance of the OPDs [22]. The higher R and D^* values of the P1:IDIC and P2:IDIC devices are 7.78×10^{11} and 7.28×10^{11} Jones, respectively, under a light intensity of 22 μW/cm^2 at −1.0 V. Even though, P1:IDIC devices showed higher R values than that of P2:IDIC devices, the lower level of J_d in P2:IDIC devices resulted in similar D^* values with that of P1:IDIC devices. We found that excessive thiophene content in P2 decreased current density in the devices with and without light irradiation. The R and D^* values were calculated from the J-V characteristics shown in **Table 2**.

The R value was investigated as a function of wavelength by measuring the external quantum efficiency (EQE) of the Polymers:IDIC device, as shown in **Figures 3a–3b**. The R values of P1:IDIC devices reached a maximum value of 0.170 A W^{-1} at –1 V under 532 nm irradiation. In the EQE graph, the efficiency of the P1:IDIC device was 18% higher at –1 V under 532 nm irradiation. The P1:IDIC device shows a higher R value than P2:IDIC device. The high R value of the P1:IDIC devices is consistent with the J-V characteristics.

Table 2. Photo-detecting properties of PCP:IDIC devices under collimated 532 nm LED light.

Active layer	P_{light} (W/cm^2)	J_d (A/cm^2)	J_{ph} (A/cm^2)	R (A/W)	D* (Jones)	Bias (V)
	2.20×10^{-5}	1.47×10^{-7}	3.72×10^{-6}	1.69×10^{-1}	7.78×10^{11}	
	1.03×10^{-4}	1.47×10^{-7}	1.58×10^{-5}	1.53×10^{-1}	7.06×10^{11}	
P1:IDIC	4.96×10^{-4}	1.47×10^{-7}	7.30×10^{-5}	1.47×10^{-1}	6.79×10^{11}	–1
	9.90×10^{-4}	1.47×10^{-7}	1.41×10^{-4}	1.43×10^{-1}	6.57×10^{11}	
	4.99×10^{-3}	1.47×10^{-7}	6.63×10^{-4}	1.33×10^{-1}	6.12×10^{11}	
	2.20×10^{-5}	7.41×10^{-8}	2.47×10^{-6}	1.12×10^{-1}	7.28×10^{11}	
	1.03×10^{-4}	7.41×10^{-8}	1.12×10^{-5}	1.09×10^{-1}	7.08×10^{11}	
P2:IDIC	4.96×10^{-4}	7.41×10^{-8}	5.37×10^{-5}	1.08×10^{-1}	7.03×10^{11}	-1
	9.90×10^{-4}	7.41×10^{-8}	1.07×10^{-4}	1.08×10^{-1}	7.02×10^{11}	
	5.00×10^{-3}	7.41×10^{-8}	5.34×10^{-4}	1.07×10^{-1}	6.94×10^{11}	

Additionally, two polymers were investigated to compare charge transport. To understand them, the Polymer:IDIC devices were measured by space charge limited current (SCLC) analysis as shown in **Figure 3c**. The hole mobilities of the P1-based and P2-based devices were measured to be 1.57×10^{-3} and 7.84×10^{-4} cm^2 V^{-1} s^{-1}, respectively. P1, which was short thiophene length, was a great performance by OPD. The hole mobility properties are shown in **Table 3**.

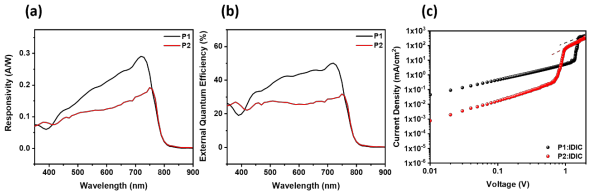

Figure 3. (a) Responsivity (R) and (b) external quantum efficiency (EQE) spectra of P1:IDIC and P2:IDIC devices as a function of wavelength at –1.0 V bias, respectively (c) hole mobility of blend film.

Table 3. Hole mobility of blend film.

Polymer	Hole mobility (cm^2/V s)
P1:IDIC	1.57×10^{-3}
P2:IDIC	7.84×10^{-4}

4. Conclusions

P1 and P2 were polymerized by Stille cross-coupling reaction of BBO-based monomer (compound 7) with thiophene (compound 5) and bithiophene (compound 8) comonomer, respectively. P2 has one more thiophene ring in a repeating unit of the polymer than P1. Both polymers showed similar green light absorption behavior with a narrow bandwidth in the region of 500−600 nm. We found that the effective π-conjugation was almost saturated at P1, and the additional thiophene ring in P2 had a negligible effect on absorbance. The bulk heterojunction OPD was fabricated by blending a conjugated polymer donor (P1 or P2) and nonfullerene acceptor (IDIC). P1:IDIC devices exhibited R of 0.169 A/W, J_d of 1.47×10^{-7} A/cm^2 and D^* of 7.78×10^{11} Jones at −1 V bias under 22 μW/cm^2 at −1.0 V, whereas P2:IDIC devices showed slightly lower R of 0.112 A/W and D^* of 7.28×10^{11} Jones at −1 V bias under 22 μW/cm^2 at −1.0 V. However, as the light intensity increases, the D^* value becomes increasingly similar. The reason is the effect of the excess thiophene unit, which maintains a low dark current.

Author Contributions

The role(s) that each author undertook should be reflected in this section. This section affirms that each credited author has had a significant contribution to the article.

All authors have read and agreed to the published version of the manuscript.

Acknowledgments

WonJo Jeong and Myeong In Kim contributed equally to this work. We would like to thank my family, The University of Hanyang Organic Nano Materials Laboratory (OEMSL) members and Professor In Hwan Jung.

Conflict of Interest

There is no conflict of interest.

Data Availability Statement

The data that support the findings of this study are available from the corresponding author upon reasonable request.

References

[1] Chow, P.C., Someya, T., 2020. Organic photodetectors for next-generation wearable electronics. Advanced Materials. 32(15), 1902045. DOI: https://doi.org/10.1002/adma.201902045

[2] Liu, J., Gao, M., Kim, J., et al., 2021. Challenges and recent advances in photodiodes-based organic photodetectors. Materials Today. 51, 475–503. DOI: https://doi.org/10.1016/j.mattod.2021.08.004

[3] Xia, K., Li, Y., Wang, Y., et al., 2020. Narrowband-absorption-type organic photodetectors for the far-red range based on fullerene-free bulk heterojunctions. Advanced Optical Mate-

rials. 8(8), 1902056.
DOI: https://doi.org/10.1002/adom.201902056

[4] Sabah, F.A., 2021. Organic polymer materials for light emitting diode applications. Organic Polymer Material Research. 3(2), 24–25.
DOI: https://doi.org/10.30564/opmr.v3i2.4348

[5] Chakraborty, S., Chatterjee, R., Bandyopadhyay, A., 2022. A brief review on fundamentals of conductive polymer (CPs). Organic Polymer Material Research. 4(1), 1–11.
DOI: https://doi.org/10.30564/opmr.v4i1.4395

[6] Luo, Y., 2023. Powering the future: Hydrogel-based soft ionic conductors energize flexible and wearable triboelectric nanogenerators. Organic Polymer Material Research. 5(1), 12–14.
DOI: https://doi.org/10.30564/opmr.v5i1.5818

[7] Wei, Y., Chen, H., Liu, T., et al., 2021. Self-powered organic photodetectors with high detectivity for near infrared light detection enabled by dark current reduction. Advanced Functional Materials. 31(52), 2106326.
DOI: https://doi.org/10.1002/adfm.202106326

[8] Kim, J., Kang, J., Jung, I.H., 2022. Synthesis and characterization of a copper (II) phthalocyanine-based dye for organic photodetectors. Bulletin of the Korean Chemical Society. 43(9), 1130–1135.
DOI: https://doi.org/10.1002/bkcs.12595

[9] Kang, J., Kim, J., Won, J.H., et al., 2021. Enhanced static and dynamic properties of highly miscible fullerene-free green-selective organic photodetectors. ACS Applied Materials & Interfaces. 13(21), 25164–25174.
DOI: https://doi.org/10.1021/acsami.1c02357

[10] Jeong, W., Kang, J., Lim, S.Y., et al., 2022. Spontaneously induced hierarchical structure by surface energy in novel conjugated polymer-based ultrafast-response organic photodetectors. Advanced Optical Materials. 10(9), 2102607.
DOI: https://doi.org/10.1002/adom.202102607

[11] Jeong, W., Kang, J., Lee, D., et al., 2023. Development of high-performance organic photodetectors by understanding origin of dark current density with synthesis of photoconductive polymers. Chemical Engineering Journal. 473, 145178.
DOI: https://doi.org/10.1016/j.cej.2023.145178

[12] Jeong, W., Kang, J., Jeong, M.K., et al., 2021. Development of low bandgap polymers for red and near-infrared fullerene-free organic photodetectors. New Journal of Chemistry. 45(24), 10872–10879.
DOI: https://doi.org/10.1039/d1nj01694f

[13] Kim, H., Kang, J., Park, J., et al., 2022. All-polymer photodetectors with n-Type polymers having nonconjugated spacers for dark current density reduction. Macromolecules. 55(21), 9489–9501.
DOI: https://doi.org/10.1021/acs.macromol.2c01769

[14] Kim, H., Kang, J., Kim, M.I., et al., 2023. Development of n-type small-molecule acceptors for low dark current density and fast response organic photodetectors. ACS Applied Materials & Interfaces. 15(49), 57545–57555.
DOI: https://doi.org/10.1021/acsami.3c11174

[15] Liu, Y., Wan, X., Wang, F., et al., 2011. Spin-coated small molecules for high performance solar cells. Advanced Energy Materials. 1(5), 771–775.
DOI: https://doi.org/10.1002/aenm.201100230

[16] Fan, Q., Su, W., Guo, X., et al., 2016. A new polythiophene derivative for high efficiency polymer solar cells with PCE over 9%. Advanced Energy Materials. 6(14), 1600430.
DOI: https://doi.org/10.1002/aenm.201600430

[17] Tlach, B.C., Tomlinson, A.L., Bhuwalka, A., et al., 2011. Tuning the optical and electronic properties of 4,8-disubstituted benzobisoxazoles via alkyne substitution. The Journal of Organic Chemistry. 76(21), 8670–8681.
DOI: https://doi.org/10.1021/jo201078w

[18] Zahran, M.K., Faheem, T.S., Abdel-Karim, A.M., et al., 2021. Enhanced optical as well as electrical properties of poly 2-acetyl pyrrole P (2-APy) for optoelectric applications. Chemical Papers. 75, 3599–3606.
DOI: https://doi.org/10.1007/s11696-021-01609-8

[19] Luponosov, Y.N., Solodukhin, A.N., Mannanov, A.L., et al., 2021. Effect of oligothiophene π-bridge length in D-π-A star-shaped small molecules on properties and photovoltaic performance in single-component and bulk heterojunction organic solar cells and photodetectors. Materials Today Energy. 22, 100863.
DOI: https://doi.org/10.1016/j.mtener.2021.100863

[20] Zhang, S., Ocheje, M.U., Huang, L., et al., 2019. The critical role of electron-donating thiophene groups on the mechanical and thermal properties of donor–acceptor semiconducting polymers. Advanced Electronic Materials. 5(5), 1800899.
DOI: https://doi.org/10.1002/aelm.201800899

[21] Lv, L., Yu, J., Sui, X., et al., 2019. Significant enhancement of responsivity of organic photodetectors upon molecular engineering. Journal of Materials Chemistry C. 7(19), 5739–5747.
DOI: https://doi.org/10.1039/c9tc00576e

[22] Yang, D., Ma, D., 2019. Development of organic semiconductor photodetectors: From mechanism to applications. Advanced Optical Materials. 7(1), 1800522.
DOI: https://doi.org/10.1002/adom.201800522

Appendix

Experimental

Synthesis of Materials

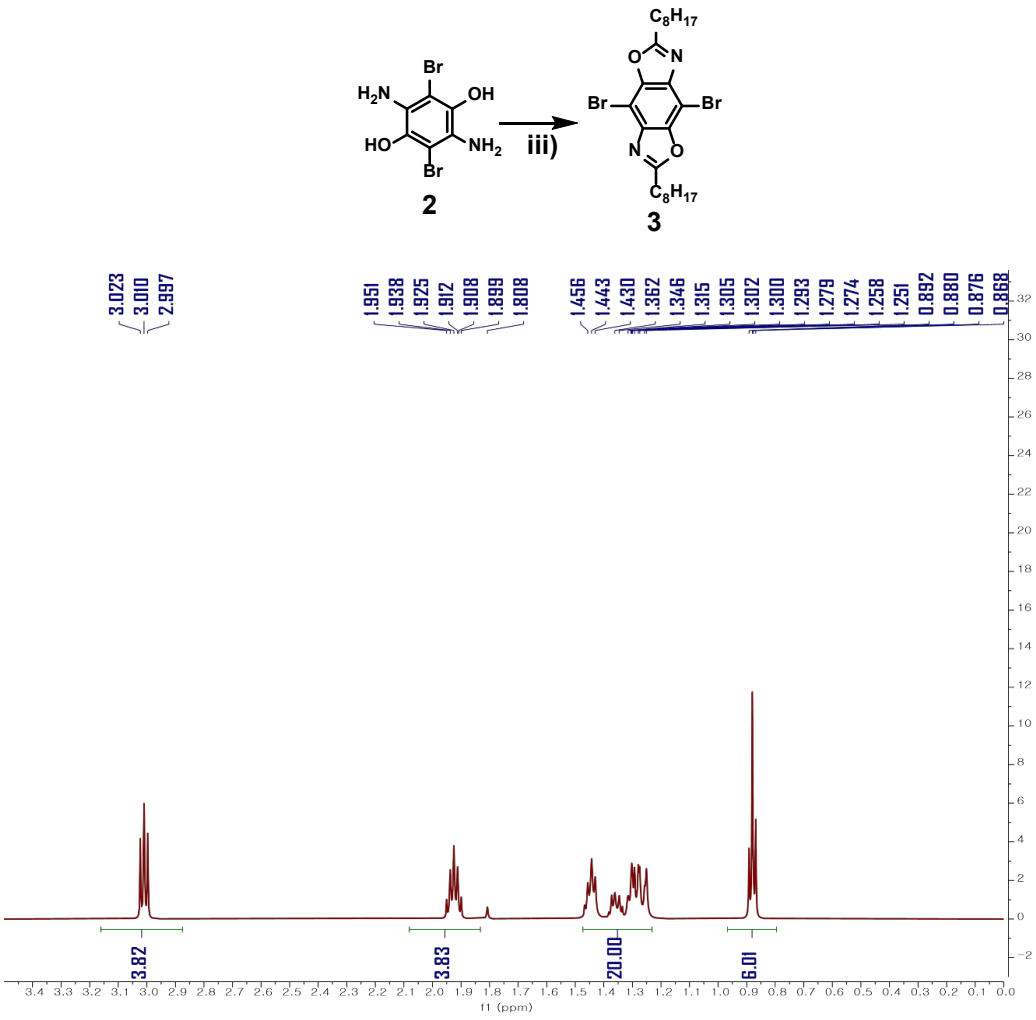

Figure S1. ^{1}H-NMR of 4,8-dibromo-2,6-dioctylbenzo[1,2-d:4,5-d']bis(oxazole).

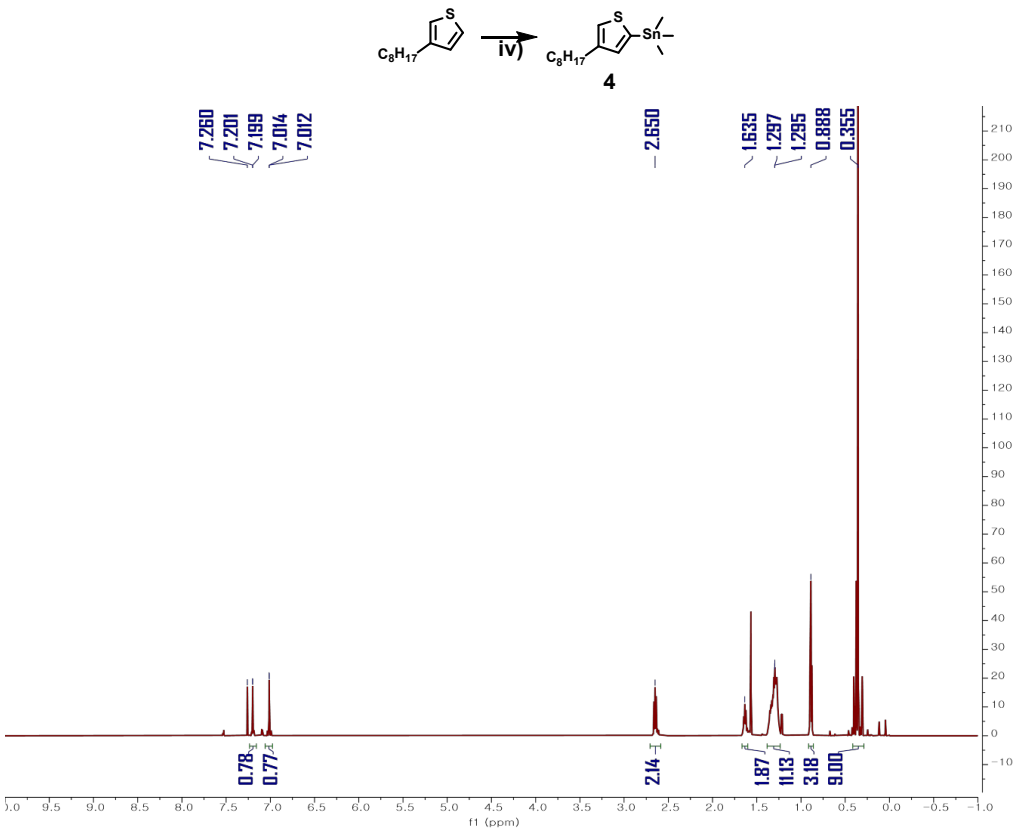

Figure S2. [1]H-NMR of 5-Trimethylstannyl-3-octylthiophene.

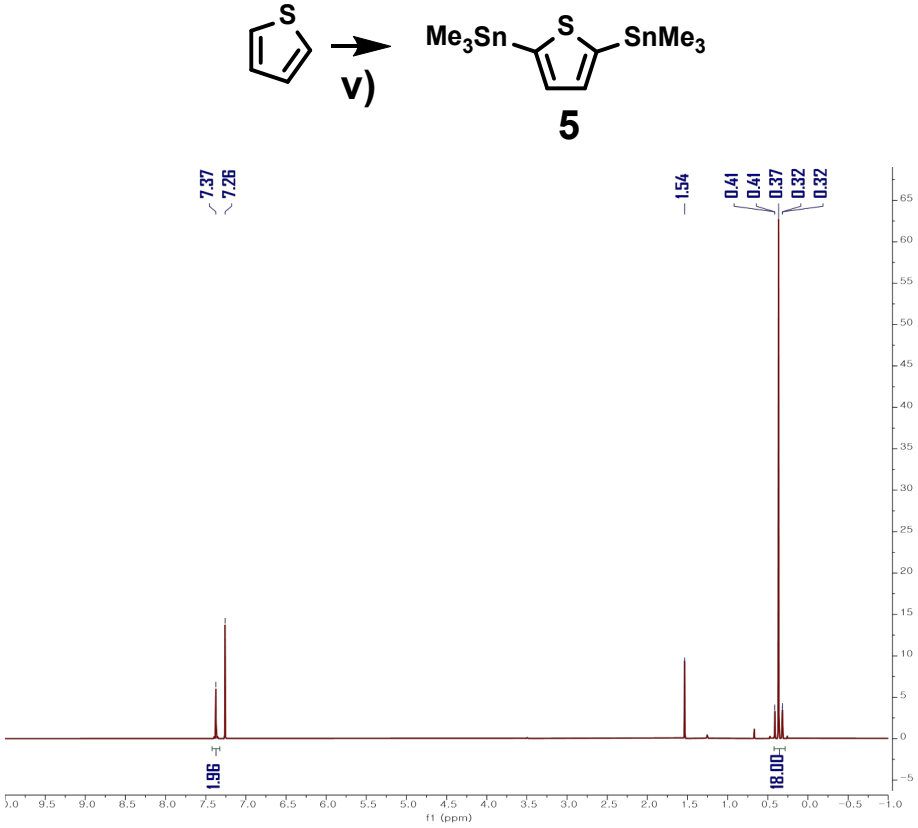

Figure S3. [1]H-NMR of 2,5-bis(trimethylstannyl)thiophene.

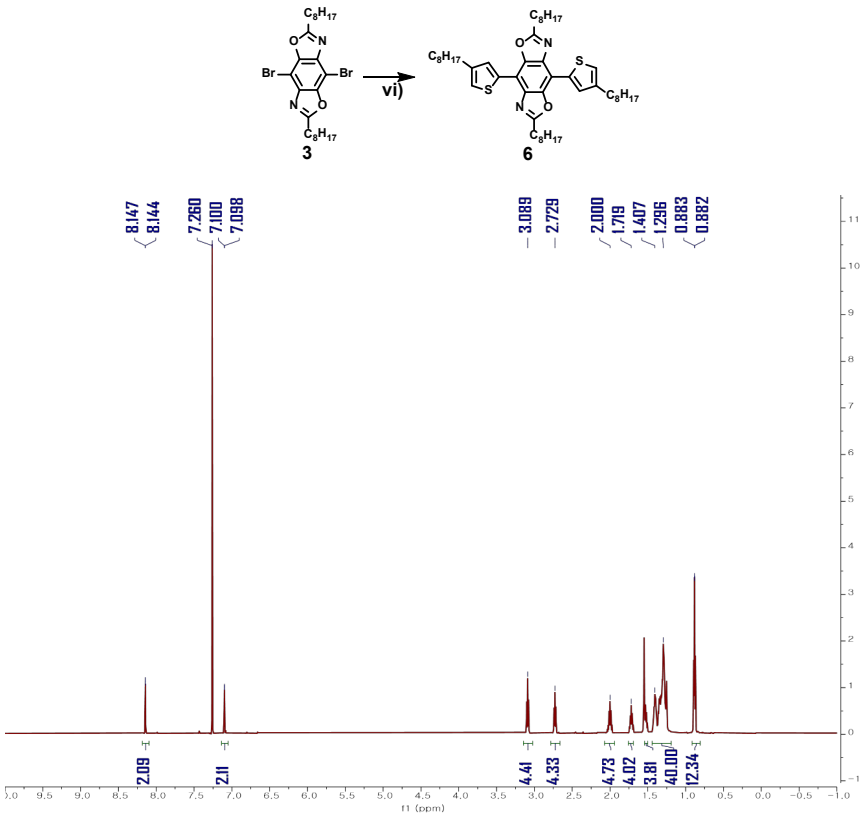

Figure S4. [1]H-NMR of 2,6-dioctyl-4,8-bis(4-octylthiophen-2-yl) benzo[1,2-d:4,5-d']bis(oxazole).

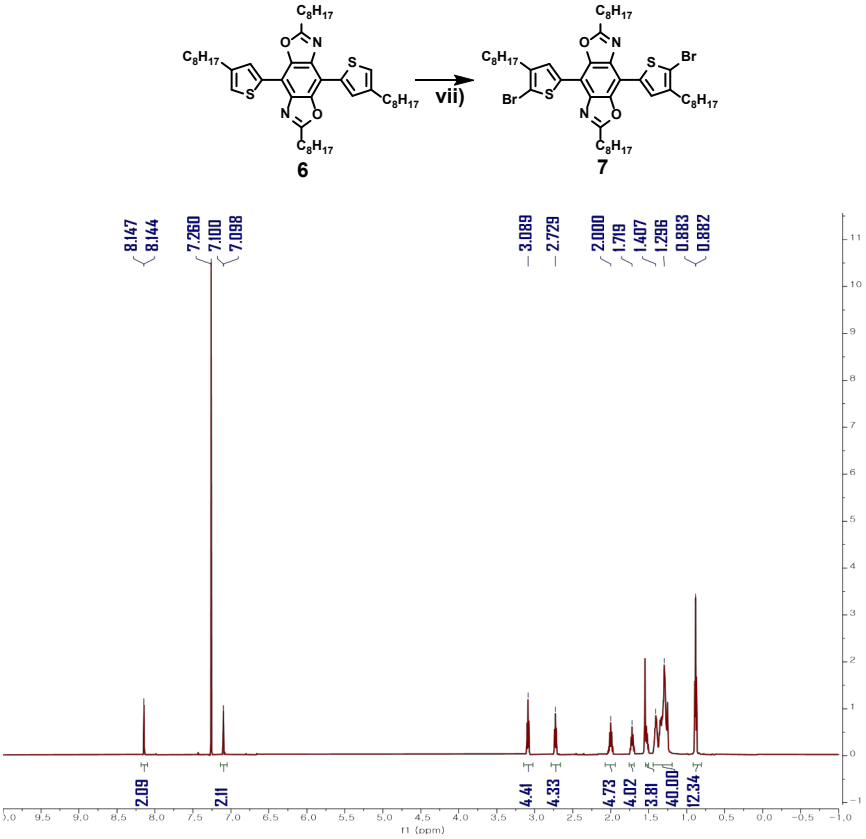

Figure S5. [1]H-NMR of 2,6-dioctyl-4,8-bis(5-bromo-4-octylthiophen-2-yl) benzo[1,2-d:4,5-d']bis(oxazole).

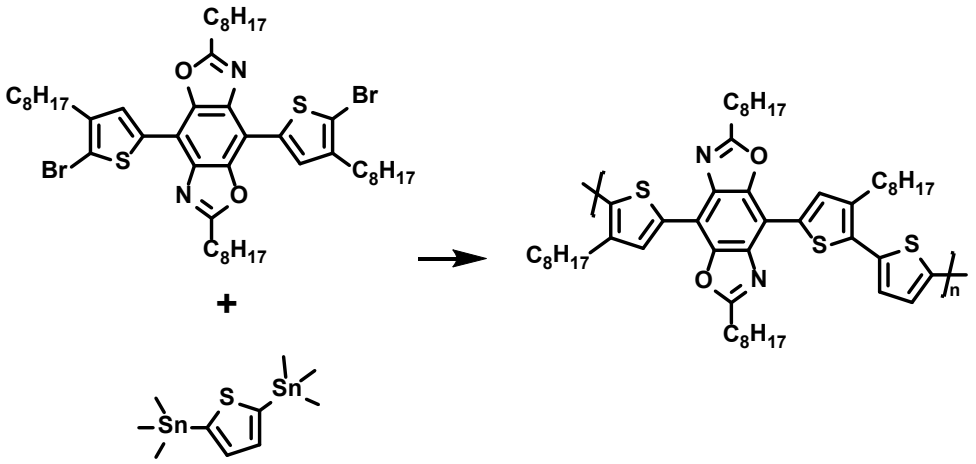

Molecular Weight Averages

Peak #	RT (min)	Mp (g/mol)	Mn (g/mol)	Mw (g/mol)	Mz (g/mol)	Mz+1 (g/mol)	PD
1	7.061	8486	5573	9553	14033	18433	1.714158

Chromatogram

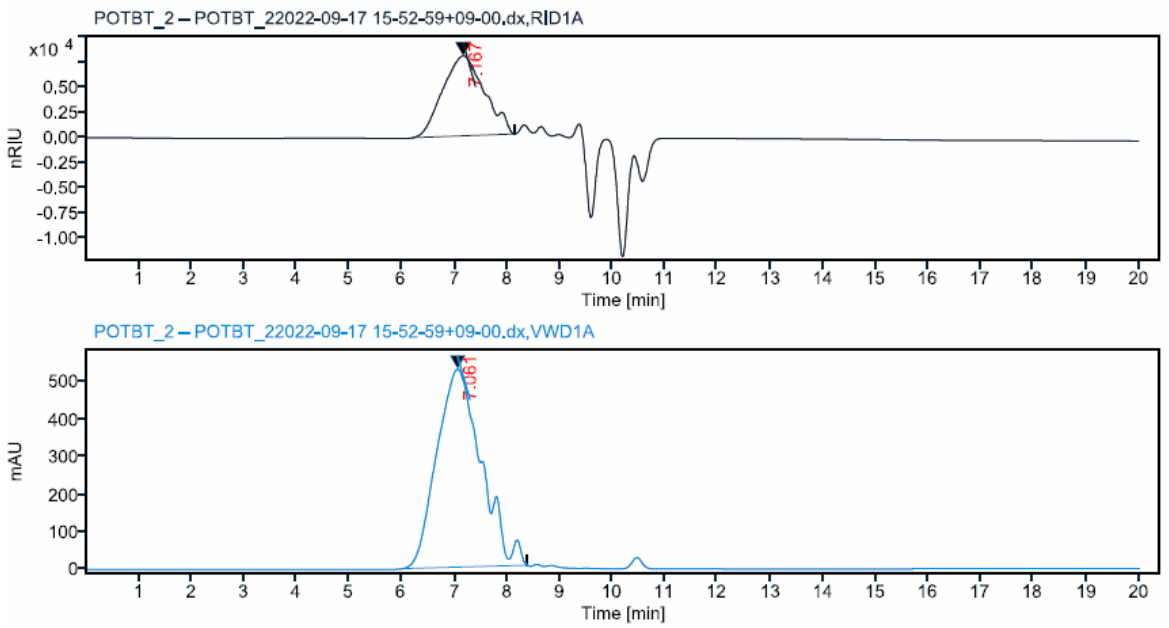

Figure S6. Gel permeation chromatography of P1 polymer.

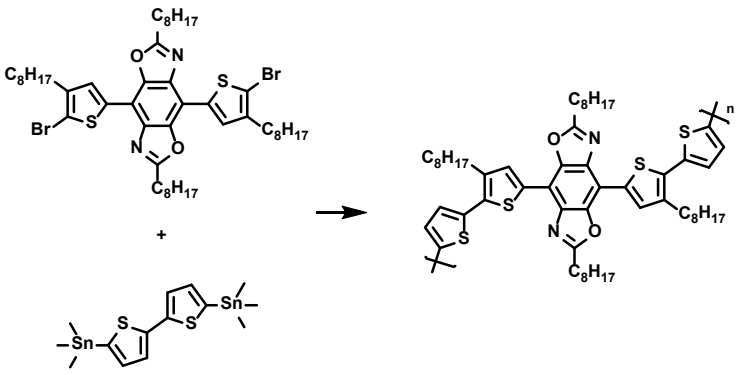

Molecular Weight Averages

Peak #	RT (min)	Mp (g/mol)	Mn (g/mol)	Mw (g/mol)	Mz (g/mol)	Mz+1 (g/mol)	PD
1	7.134	7436	4782	7228	9978	12689	1.511501

Chromatogram

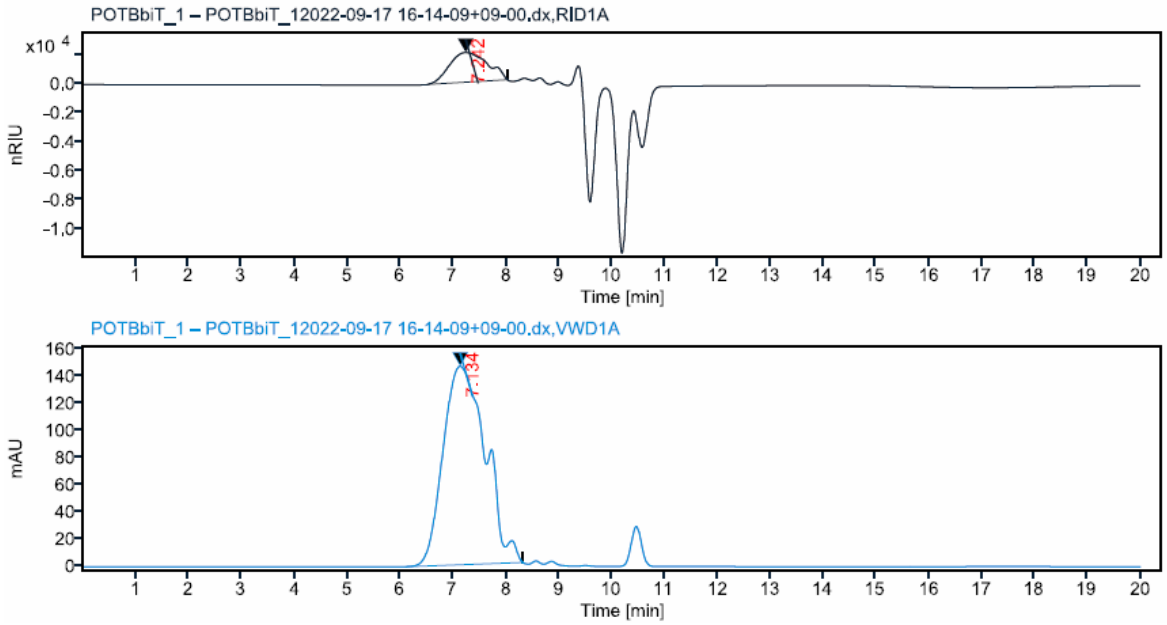

Figure S7. Gel permeation chromatography of P2 polymer.

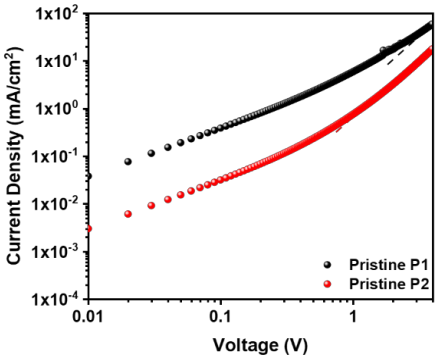

Figure S8. SCLC of pristine film.

Table S1. Hole mobility of pristine film.

cm^2/Vs	**Pristine P1**	**Pristine P2**
Hole mobility (μh)	2.25×10^{-5}	3.59×10^{-6}

Characterization of the synthesized materials

The absorption spectrum of the active layer was measured using a JASCO V-730 UV/VIS spectrometer; 1H nuclear magnetic resonance (NMR) spectra were recorded at 25 °C using a VNMRS 600 MHz spectrometer. Cyclic voltammetry measurements were performed at a scan rate of 20 mV/s using a WonATech potentiostat/galvanostat/impedance analyzer ZIVE SP1(1A), with a three-electrode cell and a 0.1 N Bu_4NBF_4 solution in acetonitrile as the electrolyte. The working electrode was coated with the polymer films by dipping them into their solutions in chloroform. The $Ag/AgNO_3$ was used as the standard electrode, and a glassy carbon working electrode. Gel permeation chromatography measurements were recorded at 35 °C using an Agilent 1260 Infinity II GPC.